JCI The Journal of Clinical Investigation

The gliotransmitter ACBP controls feeding and energy homeostasis via the melanocortin system

Khalil Bouyakdan, Hugo Martin, Fabienne Liénard, Lionel Budry, Bouchra Taib, Demetra Rodaros, Chloé Chrétien, Éric Biron, Zoé Husson, Daniela Cota, Luc Pénicaud, Stephanie Fulton, Xavier Fioramonti, Thierry Alquier

J Clin Invest. 2019. https://doi.org/10.1172/JCI123454.

Research In-Press Preview Metabolism Neuroscience

Graphical abstract

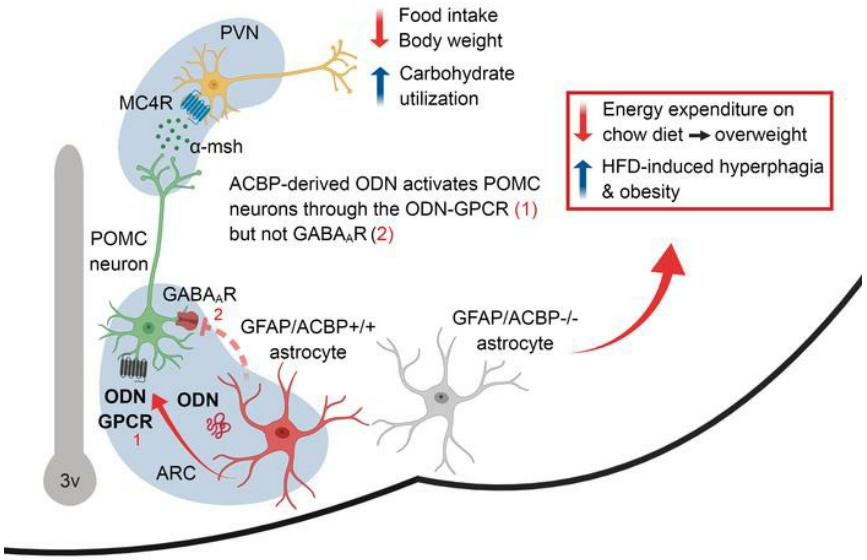

The gliotransmitter ACBP controls feeding and energy homeostasis via the melanocortin system

Khalil Bouyakdan[1], Hugo Martin[2,3], Fabienne Liénard[4], Lionel Budry[1], Bouchra Taib[1], Demetra Rodaros[1], Chloé Chrétien[4], Éric Biron[5], Zoé Husson[2,3,6], Daniela Cota[6], Luc Pénicaud[4,7], Stephanie Fulton[1], Xavier Fioramonti[2,3,4], Thierry Alquier[1,$].

[1] Centre de Recherche du Centre Hospitalier de l'Université de Montréal (CRCHUM), Montreal Diabetes Research Center, and Departments of Medicine, Pathology and Cell Biology, Biochemistry, Neurosciences and Nutrition, Université de Montréal, Montréal, QC, Canada H3T 1J4.

[2] Université de Bordeaux, INRA, NutriNeuro, 1286, F-33000, Bordeaux, France

[3] Bordeaux INP, NutriNeuro, 1286, F-33405, Talence, France

[4] Centre des Sciences du Goût et de l'Alimentation; UMR 6265 CNRS, 1324 INRA, Université de Bourgogne Franche-Comté, 21000, Dijon, France.

[5] Faculty of Pharmacy, Université Laval and Laboratory of Medicinal Chemistry, Centre de Recherche du Centre Hospitalier Universitaire de Québec (CRCHUQ), Québec, QC, Canada G1V 4G2.

[6] INSERM, Université de Bordeaux, Neurocentre Magendie, Physiopathologie de la Plasticité Neuronale, U1215, F-33000 Bordeaux, France

[7] Stromalab, CNRS ERL 5311, Université de Toulouse, Université Paul Sabatier, 31602, Toulouse, France

[$] Lead contact and to whom correspondence should be addressed: Thierry Alquier, CRCHUM-Pavillon R, 900 rue Saint-Denis, Montreal, QC, Canada, H2X0A9. Tel.: (1)514-890-8000#23628; Fax: (1)514-412-7655; E-mail: thierry.alquier@umontreal.ca

The authors have declared that no conflict of interest exists

ABSTRACT

Glial cells have emerged as key players in the central control of energy balance and etiology of obesity. Astrocytes play a central role in neural communication via the release of gliotransmitters. Acyl-CoA binding protein (ACBP)-derived endozepines are secreted peptides that modulate the $GABA_A$ receptor. In the hypothalamus, ACBP is enriched in arcuate nucleus (ARC) astrocytes, ependymocytes and tanycytes. Central administration of the endozepine octadecaneuropeptide (ODN) reduces feeding and improves glucose tolerance, yet the contribution of endogenous ACBP in energy homeostasis is unknown. We demonstrated that ACBP deletion in GFAP+ astrocytes, but not in Nkx2.1-lineage neural cells, promoted diet-induced hyperphagia and obesity in both male and female mice, an effect prevented by viral rescue of ACBP in ARC astrocytes. ACBP-astrocytes were observed in apposition with proopiomelanocortin (POMC) neurons and ODN selectively activated POMC neurons through the ODN-GPCR but not $GABA_A$, and supressed feeding while increasing carbohydrate utilization via the melanocortin system. Similarly, ACBP overexpression in ARC astrocytes reduced feeding and weight gain. Finally, the ODN-GPCR agonist decreased feeding and promoted weight loss in *ob/ob* mice. These findings uncover ACBP as an ARC gliopeptide playing a key role in energy balance control and exerting strong anorectic effects via the central melanocortin system.

INTRODUCTION

In the central nervous system, the hypothalamus is a key site for the detection and integration of circulating metabolic signals. In turn, the hypothalamus initiates appropriate neuroendocrine and behavioral responses to maintain energy homeostasis. In the arcuate nucleus (ARC) of the hypothalamus, two functionally opposing neuronal populations play a critical role in this control, the agouti-related peptide (AgRP) neurons and pro-opiomelanocortin (POMC) neurons. When activated by signals of energy sufficiency including leptin and insulin, arcuate POMC neurons release α-melanocyte-stimulating hormone that activates the melanocortin-4 receptor (MC4R) and downstream anorectic and catabolic responses (1). The importance of the melanocortin system in the etiology of obesity is underscored by several lines of evidence showing that impairments in metabolic sensing in POMC neurons lead to obesity in rodents (2-6) and that mutation in the genes coding for POMC and MC4R are the most frequent form of monogenic human obesity (7).

It is now well established that glial cells exert crucial functions in the formation, activity, and adaptation of neuronal circuits. Astrocytes are closely associated with neuronal synapses to regulate synaptic strength and neurotransmission. In line with these functions, studies implicate astrocytes in complex and fundamental behaviours such as breathing (8), sleeping (9) and feeding (10, 11).

Importantly, astrocytes have recently emerged as key players in the central response to metabolic signals and the control of energy balance (12), and obesity (13). Modulating the capacity of hypothalamic astrocytes to sense hormones and nutrients impairs glucose homeostasis (14-17) and feeding (18), and contributes to diet-induced obesity (19). Recent studies suggest that metabolites secreted by astrocytes such as lactate (20, 21), ketones (22, 23) or adenosine (10, 24) modulate the activity of hypothalamic neurocircuits. Whether and by which mechanisms astrocyte-derived signals affect the melanocortin system and downstream catabolic responses remain essentially unknown.

Astrocytes also release peptidic gliotransmitters (gliopeptides) (25) yet their contribution to the hypothalamic control of energy homeostasis is entirely unknown. Acyl-CoA binding protein (ACBP) is a highly conserved peptide secreted by cultured astrocytes (26) in response to various signals (27, 28). ACBP, also known as diazepam binding inhibitor (DBI), was initially identified in the brain as a modulator of GABA signalling by inhibiting the binding of diazepam on the $GABA_A$ receptor (29). Once secreted, ACBP

is cleaved to generate endozepines including the octadecaneuropeptide (ODN) (30). Our lab and others have shown that ACBP is expressed throughout the brain, with a particular enrichment in hypothalamic ependymocytes, tanycytes and astrocytes (31-33). Of importance, intracerebroventricular (ICV) administration of ODN reduces food intake (34) and improves glucose tolerance in rodents (33). Despite these findings, the impact of endogenous ACBP-mediated gliotransmission on feeding, energy metabolism and hypothalamic neuronal activity has not been studied. Here we used multiple gene interventions, Ca^{2+} imaging and electrophysiology to reveal the unique role of ACBP as a gliopeptide in the ARC of the hypothalamus robustly controlling feeding and energy metabolism via the melanocortin pathway.

RESULTS

Acbp gene expression is regulated by fasting but not high-fat feeding in a circadian manner

ACBP is the precursor of the anorectic peptide ODN, thus we tested whether its expression in the hypothalamus was dependent on the time of the day and nutritional status. *Acbp* mRNA level in ARC microdissections was maximal at Zeitgeber time 6 (ZT6, middle of the light cycle) and gradually decreased to its lowest level at ZT18 (Supplemental Figure 1A). *Acbp* expression was decreased by fasting at ZT6 but not ZT18 while *pomc* levels were reduced at both time points (Supplemental Figure 1B and C). Finally, *acbp* gene expression in the ARC was not affected by 3, 7 or 42 days of high-fat feeding (Supplemental Figure 1D and E). Together, these findings demonstrate that *acbp* is regulated in a circadian manner by food deprivation but not caloric excess and overweight.

Astroglial ACBP deficiency promotes diet-induced obesity

We then sought to identify the role of astroglial ACBP in energy balance using a cell-specific gene knockout approach. $ACBP^{flox/flox}GFAP^{Cre}$ ($ACBP^{GFAP}$ KO) mice were generated as we previously described (31). $ACBP^{GFAP}$ KO mice were devoid of ACBP expression in GFAP+ astrocytes and some tanycytes of the ARC and median eminence as compared to littermate control mice (Supplemental Figure 2A). Moreover, as we previously reported (31) we did not observe ACBP expression in the ependymal layer of the median eminence. *Acbp* gene expression in ARC microdissections (including the median eminence and ependymal layer) derived from chow- and high fat-fed $ACBP^{GFAP}$ KO and $GFAP^{Cre}$ control mice ($ACBP^{GFAP}$ WT)

confirmed *acbp* gene deletion (Supplemental Figure 2B). Residual *acbp* expression (10%) likely represents *acbp* expression in neurons (32) and GFAP negative astrocytes (Supplemental Figure 2A). Expectedly, *acbp* expression was reduced by half in *ACBP$^{flox/+}$GFAP^{Cre}* (ACBP^{GFAP} HET) (Supplemental Figure 2B).

Body weight was significantly increased at week 10 while energy expenditure (light phase) was reduced in chow-fed ACBP^{GFAP} KO male mice without changes, in cumulative food intake, respiratory exchange ratio (RER) and locomotor activity as compared to controls (Supplemental Figure 2C-G). Based on accumulating evidence suggesting a key role of hypothalamic astrocytes in feeding in response to leptin (18, 35) and fatty acids (19, 22), we tested whether astroglial ACBP is involved in the anorectic action of these signals. The anorectic response to central leptin was similar in ACBP^{GFAP} KO males and control littermates (Supplemental Figure 2H). In contrast, the anorectic effect of central oleate was absent in ACBP^{GFAP} KO males compared to controls (Supplemental Figure 2I). During a high-fat regimen, astroglial ACBP deficiency considerably enhanced the response to diet-induced obesity (DIO) in both male and female ACBP^{GFAP} KO mice (Figure 1A-D). Weight gain and food intake were increased in ACBP^{GFAP} KO male mice as of week 3 of the 16-week high-fat diet regimen (Figure 1A and B). Correspondingly, ACBP^{GFAP} HET male mice showed a less pronounced response to high-fat feeding suggesting a gene dosage effect. In male and female ACBP^{GFAP} KO mice, weekly food intake was increased before the onset of overweight suggesting that hyperphagia plays a causal role in the obesity prone phenotype (insets Figure 1B and D). Increased body weight gain in male ACBP^{GFAP} KO mice was not associated with changes in RER or locomotor activity (Supplemental Figure 3A and B) but with a trend towards reduced energy expenditure after 6 weeks (not shown) or 16 weeks of HFD (Supplemental Figure 3C). In contrast, female ACBP^{GFAP} KO mice had higher RER (Supplemental Figure 3D) without changes in activity and energy expenditure (Supplemental Figure 3E and F). ACBP^{GFAP} KO mice had greater fat mass (Figure 1E and Supplemental Figure 3G), with subcutaneous fat increased in males (Figure 1F) and intraperitoneal fat increased in females (Supplemental Figure 3G). Increase in fat mass was accompanied by higher plasma leptin levels (Figure 1G). A comparable enhanced weight gain in response to HFD was also observed in female mice on a mixed BL/6J-Bom genetic background (Supplemental Figure 3H). Finally, ACBP^{GFAP} KO male mice did not exhibit changes in glucose tolerance (Figure 1H and I), which could be explained by a compensatory increase in insulin secretion during the glucose tolerance test (Figure 1J) suggestive of an insulin resistance

state.

We previously reported ACBP expression in discrete ARC neurons. In addition, ACBP is highly expressed in ependymocytes and tanycytes (Supplemental Figure 2A) (32, 33), both of which are targeted by ACBP ablation in our KO model (Supplemental Figure 2A and (31)). Thus, it is possible that ACBP loss-of-function in ependymocytes and/or tanycytes may contribute to the observed phenotype. To verify this, *ACBP*$^{flox/flox}$ mice were crossed with *Nkx2.1*^{Cre} mice (ACBP$^{Nkx2.1}$ KO) in which cre is driven by Nkx2.1, a promoter expressed in hypothalamic ependymocytes, tanycytes and neurons (36, 37). As expected, ACBP protein expression was reduced in cells lining the 3rd ventricle (Supplemental Figure 4A) and *acbp* mRNA decreased by 64% in ARC microdissections (Supplemental Figure 4B). However, both male and female ACBP$^{Nkx2.1}$ KO mice on a HFD had similar body weight gain and cumulative food intake compared to control littermates (Supplemental Figure 4C and D) to suggest ACBP deficiency in hypothalamic ependymocytes, tanycytes and neurons does not influence energy balance in obesogenic conditions. Together, these results imply that pan-brain astroglial ACBP deficiency increases the susceptibility to overweight in chow-fed mice and to diet-induced hyperphagia and obesity.

***Acbp* gene rescue in ARC astrocytes prevents diet-induced obesity**

Our results suggest that astroglial ACBP plays an important role in high-fat feeding and body weight regulation, yet the pan-astroglial KO model does not permit identification of the brain region(s) involved. Based on a previous report showing that administration of the ODN C-terminal octapeptide in the ARC exerts anorectic effects similar to ICV administration (33) and on the strong ACBP expression in the ARC (32, 33), we designed an adeno-associated virus (AAV) to rescue ACBP expression selectively in GFAP+ astrocytes of the ARC of ACBP^{GFAP} KO mice (KO-ARC^{ACBP}) (38). Control mice (GFAP^{Cre} and ACBP^{GFAP} KO) were injected with a GFP-expressing AAV (Figure 2A and B) (WT-ARC^{GFP} and KO-ARC^{GFP} respectively). Expression of ACBP was partially restored in ARC astrocytes of KO-ARC^{ACBP} mice as compared to KO-ARC^{GFP} mice, but not in ependymocytes and tanycytes (Figure 2B). This partial rescue of *acbp* in the ARC (Figure 2C) prevented the decrease in *pomc* mRNA expression without affecting *agrp* mRNA levels (Figure 2D and E) and the diet-induced obesity and hyperphagia phenotype (Figure 2F and G). These findings strongly suggest that ACBP in ARC astrocytes, but not in tanycytes, ependymocytes or

extra-ARC astrocytes, is important for controlling energy balance.

Central effects of ODN on energy homeostasis rely on the melanocortin system

Our findings that astroglial ACBP in the ARC modulates high-fat feeding and body weight and a report that the anorectic effect of ODN can be offset by a melanocortin 3/4-receptor antagonist (33) suggest that the catabolic effects of ACBP could rely on the melanocortin system. First, we observed that several ACBP+ astrocytes are in close proximity to POMC neurons (Figure 3A). Second, using patch-clamp electrophysiological recordings in brain slices from POMC-eGFP mice, we found that ODN considerably increases the action potential (AP) frequency of all POMC neurons tested without affecting the firing rate of neighbouring non-POMC neurons within the ARC (Figure 3B-E).

To determine if the anorectic and metabolic effects of central ODN are dependent on the melanocortin system, ODN was administered ICV in obese MC4R KO mice and control WT mice. The dose of ODN was chosen based on a previous study in mice (34). ICV ODN decreased food intake in WT mice, an effect that lasted up to 24h (Figure 4A). In addition, ODN significantly increased RER and locomotor activity (Figure 4B and C), without affecting energy expenditure (5.05 ± 0.16 vs 5.12 ± 0.29 kcal, N=8/group, p = 0.8). The effects of central ODN were completely absent in MC4R KO mice (Figure 4D-F). To test if the ineffectiveness of ICV ODN was specific to this genetic model of obesity, similar experiments were performed in obese *ob/ob* mice in which the melanocortin system is functional. Similar to what we observed in WT mice, ICV ODN reduced feeding and increased RER in *ob/ob* mice compared to controls (Figure 4G-I). To validate the regional specificity of ODN anorectic action, we used a viral strategy to selectively overexpress ACBP in ARC GFAP+ astrocytes of C57BL/6 WT mice (WT-ARC^{ACBP}, Figure 4J). In a consistent manner, we found that ACBP overexpression in GFAP astrocytes of the ARC (Figure 4J) led to a trend towards increased *pomc* mRNA levels (Figure 4K) and was sufficient to reduce body weight gain and cumulative food intake over 10 weeks in chow-fed mice (Figure 4L and M). Together, these findings strongly suggest that the anorectic and metabolic effects of ACBP and its derived peptide ODN are mediated via the ARC melanocortin system.

ODN activates POMC neurons through a $GABA_A$ independent but ODN GPCR dependent

mechanism

ODN has been shown to act as a negative allosteric modulator of the $GABA_A$ receptor (39). Importantly, POMC neurons of the ARC receive strong inhibitory GABAergic inputs from neighboring neurons (40, 41) suggesting that ODN-induced POMC neurons activation could be due to inhibition of GABAergic inputs. Thus, the frequency and amplitude of spontaneous Inhibitory Postsynaptic Currents (sIPSC) were measured onto POMC and non-POMC neurons in brain slices from POMC-eGFP mice (42). ODN significantly decreased sIPSC frequency onto POMC- and non-POMC neurons (Figure 5A and B) without affecting sIPSC amplitude (Figure 5C), showing that ODN inhibits GABAergic inputs on ARC neurons. Importantly, these findings suggest that the decrease in GABA input is not sufficient to increase neuron activity and thus, that the selective activation of POMC neurons by ODN (Fig 3B-E) is independent of the $GABA_A$ receptor. To confirm this, brain slices were pre-treated with $GABA_A$ inhibitors to block inhibitory inputs onto POMC neurons. In these conditions, ODN was still able to increase AP frequency of POMC neurons suggesting that ODN activates these neurons independently of its action on inhibitory inputs and thus implicates another receptor (Figure 5D and E).

The second potential mechanism of action of ODN implicates the ODN G-protein coupled receptor (GPCR) coupled to phospholipase C and Ca^{2+} (43, 44). Although the ODN GPCR remains unidentified, cyclic analogs of ODN were designed based on the peptide sequence of ODN and selected for their agonist or antagonist properties (44). Application of the antagonist of ODN GPCR ($_{CD}$LOP) suggested that the anorectic action of ICV ODN is mediated through the unidentified GPCR (34). Thus, we tested whether activation of the ODN GPCR was sufficient to activate POMC neurons and reduce feeding. First, we found that treatment with the ODN GPCR agonist ($_{C}$OP) increased the firing activity of POMC neurons (Figure 5F and Supplemental Figure 5A), without affecting the firing rate of neighbouring non-POMC neurons in the ARC (Supplemental Figure 5B and C). Ca^{2+} imaging was performed in freshly dissociated hypothalamic neurons in culture which are isolated from each other (no dendrites and axons) (Supplemental Figure 5D) ruling out GABAergic inputs (45). Using this model, we observed that ODN increased intracellular Ca^{2+} oscillations in ~10% of the neurons tested (9.5% ± 1.5, Supplemental Figure 5E), a percentage compatible with the proportion of POMC neurons in mediobasal hypothalamus culture. Importantly, the ODN GPCR antagonist $_{CD}$LOP reduced both the number of ODN-responsive neurons (5% ± 1.7, $p < 0.05$, Student's *t*-

test) and the amplitude of ODN response (Supplemental Figure 5E-G), suggesting that ODN-induced neuronal activation is dependent on the ODN GPCR. Importantly, this was confirmed by electrophysiological recordings showing that the activation of POMC neurons by ODN in presence of $GABA_A$ inhibitors was reversed by the ODN receptor antagonist $_{CD}$LOP (Supplemental Figure 5H and I). Next, we observed that ICV injection of the ODN GPCR agonist $_{C}$OP decreased food intake after a fast (Figure 5G). Finally, daily ICV administration of the ODN GPCR agonist reduced feeding and body weight in *ob/ob* mice (Figure 5H and I). These results strongly suggest that ODN-induced POMC neurons activation and anorectic responses are mediated by the unidentified ODN GPCR and that activation of the receptor promotes weight loss in obese mice.

DISCUSSION

Astrocytes not only play a central role in the energy requirements of the brain but also produce and release gliotransmitters that modulate neural communication and play key roles in cognitive function (46) and behavior (47).

The present study identified the gliopeptide ACBP and its product ODN, commonly referred to as endozepines, as important hypothalamic regulators of energy balance via direct modulation of the melanocortin system. ACBP ablation in astrocytes led to increased susceptibility to diet-induced hyperphagia and obesity while viral-mediated restoration of ACBP in ARC GFAP astrocytes was sufficient to prevent this effect. Our results further show that the anorectic action of endozepines is mediated by direct activation of POMC neurons and the downstream melanocortin pathway via the ODN GPCR, whose activation reduced body weight and feeding in obese mice. Collectively, our results suggest that GPCR-mediated activation of POMC neurons by endozepines derived from hypothalamic astrocytes play a key role in feeding and body weight regulation. To our knowledge, this is the first demonstration that a gliopeptide is a key regulator of energy balance and responses to high-fat feeding. ACBP is a highly conserved protein in all eukaryotic species, found as far back as in yeast. We think that this preservation underlies the strong catabolic actions of ACBP we observe in both male and female mice on two genetic backgrounds.

Multiple genetic approaches allowed us to interrogate the role of ACBP in different cell types.

Although we and others have reported ACBP expression in neurons (32, 48), ACBP is highly enriched in non-neuronal cells of the hypothalamus including ependymocytes, astrocytes and tanycytes (31-33). Accumulating evidence suggests that tanycytes (49) and astrocytes play a key role in energy homeostasis (50). Observations of heightened DIO susceptibility in $ACBP^{GFAP}$ KO mice (loss-of-function in astrocytes, ependymocytes and tanycytes), but not in $ACBP^{Nkx2.1}$ KO mice (loss-of-function in neurons, ependymocytes and tanycytes), that were reversed by restoration of ACBP expression in ARC GFAP astrocytes firmly suggests that ACBP in ARC astrocytes regulates energy balance. We cannot rule out that the higher residual ACBP expression in the ARC of $ACBP^{Nkx2.1}$ KO vs. $ACBP^{GFAP}$ KO mice may protect from heightened DIO regardless of the cell type expressing ACBP. Nonetheless, this raises the question of the physiological role of ACBP in ependymocytes and tanycytes of the hypothalamus. Interestingly, pan-brain ACBP overexpression leads to hydrocephalus (enlargement of lateral ventricles) in mice, suggesting that ependymal ACBP may regulate cerebrospinal fluid production and/or circulation (51). In addition, ACBP is expressed in the subventricular zone, comprising ependymocytes, where it promotes neuroprogenitor proliferation via $GABA_A$ inhibition (39, 52). Additional work and genetic models will be needed to assess specifically the role of ACBP in tanycytes.

Our findings highlight novel aspects of endozepine signaling and action in the hypothalamus. Using electrophysiology, our data suggest that ODN selectively activates ARC POMC neurons and the melanocortin system to decrease feeding and stimulate carbohydrates utilization. In addition, our results strongly suggest that ODN-induced POMC neuronal activation is independent of $GABA_A$ and involves the unidentified ODN GPCR. This concept is supported by both our Ca^{2+} imaging and electrophysiology data showing that $_{CD}$LOP, an antagonist of the GPCR, decreased the number of ODN responsive neurons and the intensity of Ca^{2+} responses in dissociated hypothalamic neurons, and reversed the activation of POMC neurons by ODN in brain slices. The notion of direct and selective activation of POMC neurons has to be taken cautiously since we cannot rule out that ODN may affect different neuronal populations within other nuclei of the hypothalamus or extra-hypothalamic areas that project onto and activate POMC neurons. Nonetheless, our data at the neuronal level are consistent with a study showing that the central anorectic effect of ODN is not affected by a $GABA_A$ antagonist (34). Together, these findings demonstrate that ODN stimulation of the melanocortin system and inhibition of feeding are $GABA_A$-independent. However, ODN

decreased GABAergic inputs in all the neurons we recorded (POMC and non-POMC) suggesting a broad impact in ARC neurons that may affect the excitability of other neuronal population(s). Further investigations will be required to characterize more precisely the effect of ODN on $GABA_A$ currents and its impact on other neurocircuits in the hypothalamus.

Consistent with previous findings (34), administration of the ODN GPCR agonist $_C$OP centrally decreased feeding in WT mice in a manner similar to ICV ODN. In addition, we found that daily administration of the agonist lowered feeding and promoted body weight loss in obese *ob/ob* mice. Together, our results suggest that chronic stimulation of endozepine signalling, virally (Figure 2) or pharmacologically (Figure 5H and I), exerts potent anorectic effects in mouse models of obesity.

Our findings suggest that endozepines mostly influence energy balance by reducing food intake, while increasing locomotor activity and RER. These effects are consistent with the activation of the melanocortin system (5), however one would have expected ACBP or ODN to promote energy expenditure. It is possible that endozepines activate only a subset of POMC neurons or that higher doses may be required to affect energy expenditure.

ACBP may well exert a dual action in non-neuronal cells, both as a gliotransmitter and regulator of intracellular fatty acid metabolism. We recently showed that ACBP deficiency impairs the intracellular metabolism of unsaturated fatty acids in astrocytes (32). For this reason we cannot rule out that the unresponsiveness to the anorectic effect of central oleate and/or the obesity prone phenotype observed in $ACBP^{GFAP}$ KO mice may involve alterations of astrocyte fatty acid metabolism. However, the hyperphagia induced by ACBP deficiency in astrocytes is consistent with the anorectic effects induced by both ICV ODN (34) (Figure 4A and G) and viral-mediated expression of ACBP in ARC astrocytes (Figure 4L and M). Together, these findings provide compelling evidence that arcuate ACBP and its product ODN are anorectic gliopeptides. These findings raise the question of whether and which circulating metabolic signals stimulate the release of hypothalamic ACBP. It has been reported that glucose increases ACBP secretion in hypothalamic explants ex vivo (33). Our findings in vivo show that $ACBP^{GFAP}$ KO mice have a normal decrease in feeding in response to leptin but a dampened anorectic response to central oleate. This suggests that the release of astroglial ACBP could be stimulated by oleate to in turn inhibit feeding. Additional studies will be needed to assess this hypothesis and determine if other metabolic signals

modulate ACBP release.

At the gene level, the reduced expression of *acbp* in the ARC in response to fasting is in agreement with recent in situ hybridization data in rats (33) and is consistent with its anorectic action. Interestingly, the diurnal expression pattern of *acbp* is similar to fatty acid binding protein 7 (FABP7) (53), a brain specific isoform of FABP strongly expressed in hypothalamic astrocytes (54).

While our study demonstrates the importance of ACBP in the hypothalamus, recent findings show that ACBP is expressed in glial cells of the rat brainstem including the nucleus tractus solitarius (55), in which POMC neurons are also located. In addition, ICV injection of ODN in the 4th ventricle reduces food intake (55). This raises the possibility that brainstem ACBP may reduce feeding behavior by activating POMC neurons in the nucleus tractus solitarius. However, our viral approaches targeting ARC astrocytes suggest that hypothalamic ACBP is sufficient to reduce food intake (Figure 2G and Figure 4M). Nonetheless, the contribution of ACBP in different brain regions in short- vs. long-term regulation of food intake and the underlying mechanisms in extra-hypothalamic regions await further investigations.

More generally, it is important to mention that ACBP is expressed in several brain regions (e.g. amygdala, hippocampus) that are not commonly associated with the control of energy balance. Although, the role of ACBP in these regions is still unclear, studies suggest that endogenous ACBP may play a role in social (56) and learning behavior (57). Importantly, we recently reported that astroglial ACBP deficiency does not affect anxiety in mice (31), ruling out the possibility that DIO susceptibility in ACBP^{GFAP} KO mice is confounded by changes in anxiety-like behavior.

Altogether, our studies demonstrate that astroglial endozepines play a key role in the hypothalamic control of energy balance. Our findings, along with a study showing that Acyl-CoA binding domain-containing 7 (ACBD7, a paralog gene of ACBP) is expressed in ARC neurons and regulate feeding (58), suggest that endozepines and endozepine-like peptides are key modulators of the neurocircuits regulating energy homeostasis. These findings suggest that targeting endozepine signaling may represent a novel therapeutic avenue for obesity. More generally, our results support the emerging concept that hypothalamic astrocytes and astrocyte-derived signals play an important role in the regulation of energy balance. Undoubtedly, additional work will be required to identify the signals and pathways modulating endozepine

secretion in hypothalamic astrocytes and to identify the ODN GPCR.

METHODS

Animals: Experimental animals were bred under specific pathogen free conditions on a 12 h light – 12 h dark cycle (dark from 6:00 PM to 6:00 AM). Housing temperature was maintained at 21°C (70°F) with free access to water and standard chow diet. Cages and water were autoclaved and regular chow diet was irradiated. Cages were supplemented with nesting materials and cages were changed every two weeks. Health status was monitored via a sentinel mouse exposed to feces from the same rack.

After genotyping (4 weeks of age), experimental mice were moved to an experimental housing room on a reverse light-dark cycle (dark cycle from 10:00 AM to 10:00 PM). Mice were maintained in groups with 2-4 mice per cage until they were allocated to their experimental groups. Purchased animals were maintained in a reverse light-dark cycle for at least ten days before starting the experimentation.

For all studies, age- and sex-matched littermates were used and individually housed in a reverse light-dark cycle unless otherwise specified. Genotype, sex, age, and number of mice are indicated for each experiment in the appropriate figure legends or methods section. Upon completion of the studies, mice were anesthetised with ketamine/xylazine and blood was collected via cardiac puncture when necessary. Mice were then euthanized by decapitation before tissue collection. All mice were treatment naive at the time of study.

ACBP$^{floxl/flox}$ mice were kindly donated by Dr Susanne Mandrup (University of Southern Denmark, Odense, Denmark) (31, 59) and were backcrossed at least 8 generations on the C57BL/6J genetic background (C57BL/6J, 000664). Female *ACBP*$^{flox/flox}$ mice on the C57BL/6J background were bred with male mice expressing Cre recombinase under the mouse glial fibrillary acidic protein (GFAP) promoter (B6.Cg-Tg(Gfap-cre)73.12Mvs/J, 012886), obtained from the Jackson Laboratory (Bar Harbor, ME). *ACBP*$^{+/+}$*;Cre* (WT), *ACBP*$^{flox/+}$*;Cre* (HET) and *ACBP*$^{flox/flox}$*;Cre* (KO) were obtained by breeding female *ACBP*$^{flox/+}$ with male *ACBP*$^{flox/+}$*;Cre* to obtain littermates of all genotypes. Some studies (Supplemental Figures) were performed on ACBP KO animals (on a mixed C57BL/6J and Bom background) obtained by breeding *ACBP*$^{flox/flox}$ mice, on the original C57BL/6 Bom genetic background , with GFAP-Cre or Nkx2.1-Cre mice (C57BL/6J-Tg(Nkx2-1-cre)2Sand/J, 008661).

Male MC4R KO and control wild type (WT) mice (B6; 129S4-Mc4r^{tm1Lowl}/J, 006414), POMC-eGFP mice (C57BL/6J-Tg(Pomc-EGFP)1Low/J, 009593) and *ob*/*ob* (B6.Cg-*Lep*^{ob}/J, 000632) mice were purchased from the Jackson Laboratory (6-10 weeks old). Male POMC-eGFP hemizygous mice were bred with C57BL/6J WT females from the same genetic background to produce experimental animals.

Astrocyte specific overexpression of ACBP

Ten to twelve week old male C57BL/6J WT mice were injected bilaterally in the arcuate nucleus (ARC) as previously described (38) according to stereotaxic coordinates (from bregma: -1.5 mm antero-posterior, 0.15 mm lateral and -5.9 mm dorso-ventral from the dura) with 400 nL per side of either control (AAV5-GFAP(0.7)-GFP, Vector Biolabs, Malvern, PA USA) or overexpressor (AAV5-GFAP(0.7)-mACBP-IRES-GFP-WPRE, Vector Biolabs, Malvern, PA USA) virus at a concentration of 2.6x10^{9} GC/µL (1.04x10^{9} GC per side) to generate WT-ARC^{GFP} and WT-ARC^{ACBP} mice. Mice were allowed to recover for 1 week before the beginning of the study. Placement and efficacy of viral expression of ACBP was measured by qPCR on ARC and VMH microdissections. Mice that did not show at least a 10% increase in ACBP expression in the ARC compared to WT-ARC^{GFP} controls were excluded from the study.

Astrocyte specific rescue of ACBP

Ten to twelve week old male ACBP^{GFAP} WT (GFAP-Cre) and ACBP^{GFAP} KO mice were injected bilaterally in the ARC according to stereotaxic coordinates (from bregma: -1.5 mm antero-posterior, 0.15 mm lateral and -5.9 mm dorso-ventral from the dura) with 400 nL per side of either control (AAV5-GFAP(0.7)-GFP Vector Biolabs, Malvern, PA USA) or overexpressor (AAV5-GFAP(0.7)-mACBP-IRES-GFP-WPRE Vector Biolabs, Malvern, PA USA) virus at a concentration of 2.6x10^{9} GC/µL (1.04x10^{9} GC per side) to generate WT-ARC^{GFP}, KO-ARC^{GFP} and KO-ARC^{ACBP} mice. Mice were allowed to recover for 3 weeks before the onset of the study. Placement and efficacy of viral expression of ACBP was measured by qPCR on ARC and VMH microdissections. Mice that did not show at least a 10% increase in ACBP expression in the ARC compared to KO-ARC^{GFP} controls were excluded from the study.

In vivo studies

High fat diet studies

Five to six week old mice (ACBP^{GFAP} and ACBP$^{Nkx2.1}$ KO, HET and control littermates) were individually housed and fed either chow during 12 weeks or a high fat diet (HFD) (Modified AIN-93G purified rodent diet

with 50 % Kcal from fat derived from palm oil, Dyets, Bethlehem, PA, USA) during 16 weeks. Five to six week old mice on a mixed BL/6J-Bom background ($ACBP^{GFAP}$ and $ACBP^{Nkx2.1}$ KO, HET and control $ACBP^{flox/flox}$ littermates) were individually housed and fed with a HFD (F3282, 60% Kcal from fat, Bioserv, Flemington, NJ, USA) during 12 weeks. Body weight and food intake were measured weekly from 9:00 AM to 10:00 AM at the end of the light cycle. WT-ARC^{GFP} and WT-ARC^{ACBP} mice were individually housed following surgery and fed on chow. Food intake was measured weekly from 9:00 AM to 10:00 AM during 10 weeks starting one week after the surgery. WT-ARC^{GFP}, KO-ARC^{GFP} and KO-ARC^{ACBP} mice were individually housed following surgery and fed with the HFD. Food intake was measured weekly from 9:00 AM to 10:00 AM during 12 weeks starting three weeks after surgery.

Metabolic cages

Respiratory exchange ratio (RER), energy expenditure and locomotor activity were measured using indirect calorimetry in Comprehensive Lab Animal Monitoring System metabolic cages (CLAMS, Columbus Instruments International, Columbus, OH, USA). Animals were single housed in CLAMS apparatus at 21°C (70°F) in a dark-light cycle matching their housing conditions during 24 h for acclimation followed by 48 h of measurement. Energy expenditure was normalized by lean mass.

Glucose tolerance

Experimental mice were food-deprived during 5 h with *ad libitum* access to water. A bolus of glucose (1.5 g/kg) was administered via an intraperitoneal (IP) injection and glycaemia was measured from blood sampled at the tail vein using a Accu-chek Performa glucometer at T0 (before injection), 15, 30, 60 and 90 min. Tail vein blood samples were collected via a capillary for insulin assays.

Body composition analysis

Total fat and lean mass were assessed using a nuclear echo magnetic resonance imaging (MRI) whole-body composition analyzer. Intraperitoneal (perigonadal) and subcutaneous (inguinal) fat pads were collected and weighed using an analytical scale (Sartorius, Göttingen, Germany).

Intracerebroventricle cannula implantation

Male mice were anaesthetised with isoflurane and placed on a stereotaxic apparatus (Kopf instrument, Tujunga, CA, USA). Animals were implanted with a guide cannula (Plastics One, Roanoke, VA, USA) into the right lateral ventricle according to stereotaxic coordinates (from bregma: -0.5 mm antero-posterior, +1

mm lateral and -2.1 mm dorso-ventral from the dura). Cannulated mice were allowed to recover for a week before intracerebroventricular (ICV) administration of angiotensin II (40 ng in 2 µl) to verify placement. Mice that did not exhibit repeated bouts of drinking within the first 5 min were excluded from the study.

Intracerebroventricular injections

WT, MC4R KO and *ob/ob* male mice were separated into two groups. A first cohort was fasted during 16 h starting at 5:00 PM (7 h after the start of the dark cycle) before ICV administration of either freshly reconstituted ODN (100 ng in 2 µl; Phoenix pharmaceuticals, Burlingame, CA, USA) or saline at 9:00 AM, 1 h before the dark cycle. Access to food was restored 30 min after ICV injection and food intake was measured at 1, 2, 4, 6, 12 and 24 h post injection. A second cohort of animals was single housed in metabolic cages (CLAMS) during 24 h for acclimation and were administered with either freshly reconstituted ODN (100 ng in 2 µl) or saline 1 h before the onset of the dark cycle and monitored for 24 h.
Male C57BL/6 WT mice were fasted during 16 h starting at 5:00 PM (7 h after the start of dark cycle) before ICV administration of either freshly reconstituted ODN receptor agonist cyclo$_{1\text{-}8}$OP ($_{C}$OP, 50 ng in 2 µL) prepared by standard Fmoc solid-phase peptide synthesis as previously described (44) or saline at 9:00 AM, 1 h before the dark cycle. Access to food was restored 30 min after ICV injection and food intake was measured at 1, 2, 4, 6, 12 and 24 h post injection.
ob/ob male mice received daily ICV administration of either freshly reconstituted ODN receptor agonist $_{C}$OP (34) (50 ng in 2 µL) or saline control at 9:00 AM, 1 h before the dark cycle during 4 days. Body weight and food intake were measured daily.

Ex vivo studies

Electrophysiological recordings

Electrophysiological recordings were performed as previously described (42). Non fasted 6-10 week old POMC-eGFP mice (C57BL/6J-Tg(Pomc-EGFP)1Low/J, stock number 009593) were intracardially perfused under anesthesia (pentobarbital 120 mg/kg) with an ice-cold oxygenated (95% O_2/5% CO_2) perfusion solution that contained (in mM) 200 sucrose, 28 $NaHCO_3$, 2.5 KCl, 7 $MgCl_2$, 1.25 NaH_2PO_4, 0.5 $CaCl_2$, 1 L-ascorbate, and 8 D-glucose (pH 7.4) . The brain was quickly removed and immersed in the same ice-cold oxygenated perfusion solution. Three 250 µM coronal slices containing the ARC were performed with a vibroslice (Leica VT1000S, Leica, Wetzlar, Germany) and placed for 1 h at room temperature in an

oxygenated recovery ACSF solution containing (in mM): 118 NaCl, 5 KCl, 1 $MgCl_2$, 25 $NaHCO_3$, 1.2 NaH_2PO_4, 1.5 $CaCl_2$, 5 HEPES, 2.5 D-glucose and 15 sucrose (osmolarity adjusted to 310 mOsM with sucrose, pH 7.4). After recovery, slices were perfused with the same ACSF oxygenated media in a recording chamber placed under a microscope (Nikon EF600, Nikon, Tokyo, Japan) outfitted for fluorescence and IR-DIC videomicroscopy. Viable ARC POMC neurons were visualized with a fluorescence video camera (Nikon, Tokyo, Japan). For cell-attached recordings, borosilicate pipettes (4-6 MΩ; 1.5 mm OD, Sutter Instrument, Novato, CA, USA) were filled with filtered extracellular medium. For measures of POMC neurons firing rate in response to ODN (1nM), AP frequency was quantified in POMC and non-POMC neurons before (control; over the last 60 sec before ODN application), during (1 nM ODN 3-5 min, over the last 60 sec of ODN application) and after (reversal 10 min, over 60 sec, 10 min after ODN application) ODN application at room temperature. For the measurement of POMC neurons firing rate in presence of GABAergic inhibitors (bicuculine and picrotoxin), slices were perfused with the glutamate receptors inhibitors CNQX (cyanquixaline, 20 µM) and D-APV (50 µM) to prevent POMC neurons over-excitation (Fig 5). For the measurement of spontaneous inhibitory post-synaptic currents (sIPSC) under whole-cell voltage-clamp recordings, pipettes were filled with a cesium-chloride solution containing (in mM): 140 CsCl, 3.6 NaCl, 1$MgCl_2$, 10 HEPES, 0.1 Na_4EGTA, 4 Mg-ATP, 0.25 Na-GTP (290 mOsm, pH 7.3). Recordings were made using a Multiclamp 700B amplifier, digitized using the Digidata 1440A interface and acquired at 2 kHz using pClamp 10.5 software (Axon Instruments, Molecular Devices, Sunnyvale, CA, USA). Pipettes and cell capacitances were fully compensated. After a stable baseline was established, 1 nM of ODN or 2 nM of $_C$OP was perfused for 5-10 minutes. POMC neurons' action potential or IPSCs frequency were measured over the last minute of the ODN or $_C$OP perfusion and compared with the respective frequency measured 1 minute before the perfusion.

Calcium imaging

Mediobasal hypothalamic neurons were prepared from 3-4 weeks-old Wistar rats as described previously (45). Cells were loaded with Fura-2/acetoxymethyl ester (0.5 µM; Fura-2/AM; Molecular Probes, Eugene, OR, USA) for 20 min at 37°C in Hanks buffer balanced salt solution (containing (in mM): 25 HEPES, 121 NaCl, 4.7 KCl, 1.2 $MgSO_4$, 1.2 KH_2PO_4, 5 $NaHCO_3$, 2 $CaCl_2$, 2.5 D-glucose; pH 7.4)). Fura-2 fluorescence images were acquired every 10 sec by alternating excitation at 340 and 380 nm and emissions (420–600

nm) with a CDD camera coupled to Live Acquisition software (TiLL Photonics). Changes in intracellular calcium levels ($[Ca^{++}]_i$) were monitored in cells held at 2.5 mM glucose in response to ODN (1 nM) with or without the ODN receptor antagonist $cyclo_{1-8}[dLeu^5]OP$ ($_{CD}LOP$) (10 nM) prepared by standard Fmoc solid-phase peptide synthesis based on a previous study (44). Values for the 340/380 nm fluorescence ratio, representative of $[Ca^{2+}]_i$, were obtained after correction for background fluorescence values. Changes in $[Ca^{2+}]_i$ were quantified by calculating the integrated area under the curve (AUC) of each ODN response with the TiLL Photonics software. Neurons were considered as ODN-responsive neurons if the increase in $[Ca^{2+}]_i$ occurred between 2 and 10 minutes of treatment, had an amplitude > 0.2 (Δratio 340/380), lasted at least 30 seconds and was transient. At the end of each recording, neuronal excitability was verified by measuring Ca^{2+} response to 50 mM KCl. Neurons not responding to KCl were excluded from the analysis. Analysis of each experiment was obtained from at least 3 independent cultures prepared from at least 2 animals.

Immunofluorescence

Male mice were perfused intracardially with 4% paraformaldehyde under ketamine/xylazine anaesthesia. The brains were post-fixed 3 h in 4% paraformaldehyde, cryopreserved in 20% sucrose, and cryosectionned at 30 µm using a sliding microtome (SM 2000R Leica, Wetzlar, Germany). Sections were blocked and incubated with primary antibodies overnight at 4°C followed by 2 h incubation at 22°C with secondary antibodies. Sections were mounted and imaged with a Zeiss fluorescent microscope (Carl Zeiss AG, Jena, Germany). Primary antibodies used were anti-ACBP/DBI (1:600; DBI-Rb-Af300, Frontier Institute, Hokkaido, Japan) and anti-ACBP (1:200, polyclonal antibody, kind gift of J. Knudsen and S. Mandrup), and anti-glial fibrillary acidic protein (1:1000, Mab360, Millipore Corporation, Bedford, MA, USA). Secondary antibodies were Alexa Fluor® 546 Goat Anti-Rabbit IgG, A-11035 and Alexa Fluor® 488 Goat Anti-Mouse IgG, A-11001 (1:1000, Life Technologies, Carlsbad, CA, USA).

Real-time PCR

Real-time PCR was performed as previously described (32). Fresh ARC microdissections that include the median eminence and the ependymal layer, or VMH microdissections, were immediately frozen on dry ice before RNA extraction using the TRIzol method (Life Technologies, Carlsbad, CA, USA). RNA concentration was quantified spectrophotometrically using a NanoDrop 2000 (Thermofisher, Waltham, MA,

USA) and 1 µg of total RNA was reverse-transcribed by M-MuLV reverse transcriptase (Life Technologies, Carlsbad, CA, USA) with random hexamers following the manufacturer's conditions. The reaction mix was then diluted fivefold before use. Quantitative gene expression was measured from 1:10 cDNA dilutions. Real-time PCR was performed using the QuantiFast SYBR Green PCR kit (Qiagen, Valencia, CA, USA) according to the manufacturer's guidelines on a Corbett Rotor-Gene 6000. Data were analyzed using the standard curve method and normalized to *actin*, *cyclophillin* or *18s* RNA expression levels.

Blood chemistry

Plasma insulin and leptin levels were measured in blood samples collected at sacrifice or during the GTT in chow- or HFD-fed ACBP^{GFAP} WT and ACBP^{GFAP} KO male mice. Insulin and leptin assays were performed by the core metabolic phenotyping platform of the CRCHUM using commercially available ELISA kits.

Statistical analysis

All statistical analysis were performed using GraphPad Prism software. Intergroup comparisons were performed by ANOVA with Bonferroni post hoc tests or Student's *t*-test (two tailed) as described in figure legends. $p < 0.05$ was considered significant. Data are expressed as means ± SEM.

Study approval

All procedures using animals were reviewed and approved by the institutional animal care and use committee (Comité Institutionnel de Protection de Animaux, protocol #CM16007TAs) of Centre de Recherche du Centre Hospitalier de l'Université de Montréal (CRCHUM) and the French Ministry of Research and the institutional ethic committees of Université de Bourgogne (C2EA # 105) and Université de Bordeaux (C2EA # 50).

AUTHORS CONTRIBUTIONS

KB, BT and LB helped with colonies management, mouse models validation and performed feeding, metabolic, qPCR and immunofluorescence studies. CC performed Ca^{2+} imaging. DR performed colonies genotyping, GTT, ICV and AAV injections. DC and ZH performed AAV injections in POMC-Cre mice. FL, HM and XF performed electrophysiological recordings. EB synthesized the agonist and antagonist. SF and LP contributed to conceptualization and results interpretation. KB, XF, SF and TA analyzed results and prepared the manuscript.

ACKNOWLEDGEMENTS

We are grateful to S. Mandrup for the ACBP floxed mice. Authors are thankful to A. Lefranc, L. Decocq and A. Mathou for animal care. We thank the CRCHUM rodent metabolic phenotyping core facility for their help with CLAMS and MRI studies and the cell biology and physiology core facility for hormone assays. We thank S. Luquet (Université Paris-Diderot) for insightful discussions. We are grateful to S. Audet (CRCHUM) for his help with qPCR. This work was supported by grants from the Canadian Institutes of Health Research (MOP115042 and PJT153035 to TA), Marie Curie Foundation (CIG NeuROSenS PCIG09-GA-2011-293738 to XF), Société Francophone du Diabète and Diabète Québec (to TA) and Réseau cardiométabolique, diabète & obésité from Fonds de Recherche Québec-Santé (CMDO-FRQS to TA and XF) and from INSERM, Agence Nationale Recherche ANR-13-BSV4-0006, ANR-18-CE14-0029-02 (to DC) and ANR-10-LABX-43 Labex BRAIN (to DC and XF). HM and CC were supported by a fellowship from the department AlimH INRA and the Région Nouvelle Aquitaine or Région Bourgogne, respectively. XF and LP were also supported by the PARI Région Bourgogne. TA, SF and EB were supported by a salary award from FRQS. KB and BT were supported by a fellowship from Diabète Québec and LB by a fellowship from Diabetes Canada.

DISCLOSURES

Authors have no conflict of interest to declare.

REFERENCES

1. Krashes MJ, Lowell BB, and Garfield AS. Melanocortin-4 receptor-regulated energy homeostasis. *Nat Neurosci.* 2016;19(2):206-19.
2. Coppari R, Ichinose M, Lee CE, Pullen AE, Kenny CD, McGovern RA, Tang V, Liu SM, Ludwig T, Chua SC, Jr., et al. The hypothalamic arcuate nucleus: a key site for mediating leptin's effects on glucose homeostasis and locomotor activity. *Cell Metab.* 2005;1(1):63-72.
3. Claret M, Smith MA, Batterham RL, Selman C, Choudhury AI, Fryer LG, Clements M, Al-Qassab H, Heffron H, Xu AW, et al. AMPK is essential for energy homeostasis regulation and glucose sensing by POMC and AgRP neurons. *The Journal of clinical investigation.* 2007;117(8):2325-36.
4. Parton LE, Ye CP, Coppari R, Enriori PJ, Choi B, Zhang CY, Xu C, Vianna CR, Balthasar N, Lee CE, et al. Glucose sensing by POMC neurons regulates glucose homeostasis and is impaired in obesity. *Nature.* 2007;449(7159):228-32.
5. Berglund ED, Vianna CR, Donato J, Jr., Kim MH, Chuang JC, Lee CE, Lauzon DA, Lin P, Brule LJ, Scott MM, et al. Direct leptin action on POMC neurons regulates glucose homeostasis and hepatic insulin sensitivity in mice. *The Journal of clinical investigation.* 2012;122(3):1000-9.
6. Hill JW, Elias CF, Fukuda M, Williams KW, Berglund ED, Holland WL, Cho YR, Chuang JC, Xu Y, Choi M, et al. Direct insulin and leptin action on pro-opiomelanocortin neurons is required for normal glucose homeostasis and fertility. *Cell Metab.* 2010;11(4):286-97.
7. Oswal A, and Yeo GS. The leptin melanocortin pathway and the control of body weight: lessons from human and murine genetics. *Obes Rev.* 2007;8(4):293-306.
8. Gourine AV, Kasymov V, Marina N, Tang F, Figueiredo MF, Lane S, Teschemacher AG, Spyer KM, Deisseroth K, and Kasparov S. Astrocytes control breathing through pH-dependent release of ATP. *Science.* 2010;329(5991):571-5.
9. Pelluru D, Konadhode RR, Bhat NR, and Shiromani PJ. Optogenetic stimulation of astrocytes in the posterior hypothalamus increases sleep at night in C57BL/6J mice. *Eur J Neurosci.* 2016;43(10):1298-306.
10. Yang L, Qi Y, and Yang Y. Astrocytes control food intake by inhibiting AGRP neuron activity via adenosine A1 receptors. *Cell Rep.* 2015;11(5):798-807.
11. Chen N, Sugihara H, Kim J, Fu Z, Barak B, Sur M, Feng G, and Han W. Direct modulation of GFAP-expressing glia in the arcuate nucleus bi-directionally regulates feeding. *Elife.* 2016;5:e18716.
12. Douglass JD, Dorfman MD, and Thaler JP. Glia: silent partners in energy homeostasis and obesity pathogenesis. *Diabetologia.* 2017;60(2):226-36.
13. Thaler JP, Yi CX, Schur EA, Guyenet SJ, Hwang BH, Dietrich MO, Zhao X, Sarruf DA, Izgur V, Maravilla KR, et al. Obesity is associated with hypothalamic injury in rodents and humans. *The Journal of clinical investigation.* 2012;122(1):153-62.
14. Chari M, Yang CS, Lam CK, Lee K, Mighiu P, Kokorovic A, Cheung GW, Lai TY, Wang PY, and Lam TK. Glucose transporter-1 in the hypothalamic glial cells mediates glucose sensing to regulate glucose production in vivo. *Diabetes.* 2011;60(7):1901-6.
15. Marty N, Dallaporta M, Foretz M, Emery M, Tarussio D, Bady I, Binnert C, Beermann F, and Thorens B. Regulation of glucagon secretion by glucose transporter type 2 (glut2) and astrocyte-dependent glucose sensors. *The Journal of clinical investigation.* 2005;115(12):3545-53.
16. Garcia-Caceres C, Quarta C, Varela L, Gao Y, Gruber T, Legutko B, Jastroch M, Johansson P, Ninkovic J, Yi CX, et al. Astrocytic Insulin Signaling Couples Brain Glucose Uptake with Nutrient Availability. *Cell.* 2016;166(4):867-80.
17. Guillod-Maximin E, Lorsignol A, Alquier T, and Penicaud L. Acute intracarotid glucose injection towards the brain induces specific c-fos activation in hypothalamic nuclei: involvement of astrocytes in cerebral glucose-sensing in rats. *Journal of neuroendocrinology.* 2004;16(5):464-71.
18. Kim JG, Suyama S, Koch M, Jin S, Argente-Arizon P, Argente J, Liu ZW, Zimmer MR, Jeong JK, Szigeti-Buck K, et al. Leptin signaling in astrocytes regulates hypothalamic neuronal circuits and feeding. *Nat Neurosci.* 2014;17(7):908-10.
19. Gao Y, Layritz C, Legutko B, Eichmann TO, Laperrousaz E, Moulle VS, Cruciani-Guglielmacci C, Magnan C, Luquet S, Woods SC, et al. Disruption of Lipid Uptake in Astroglia Exacerbates Diet-Induced Obesity. *Diabetes.* 2017;66(10):2555-63.
20. Lam TK, Gutierrez-Juarez R, Pocai A, and Rossetti L. Regulation of blood glucose by hypothalamic

pyruvate metabolism. *Science.* 2005;309(5736):943-7.
21. Clasadonte J, Scemes E, Wang Z, Boison D, and Haydon PG. Connexin 43-Mediated Astroglial Metabolic Networks Contribute to the Regulation of the Sleep-Wake Cycle. *Neuron.* 2017;95(6):1365-80 e5.
22. Le Foll C, Dunn-Meynell AA, Miziorko HM, and Levin BE. Regulation of hypothalamic neuronal sensing and food intake by ketone bodies and fatty acids. *Diabetes.* 2014;63(4):1259-69.
23. Le Foll C, Dunn-Meynell AA, Miziorko HM, and Levin BE. Role of VMH ketone bodies in adjusting caloric intake to increased dietary fat content in DIO and DR rats. *Am J Physiol Regul Integr Comp Physiol.* 2015;308(10):R872-8.
24. Sweeney P, Qi Y, Xu Z, and Yang Y. Activation of hypothalamic astrocytes suppresses feeding without altering emotional states. *Glia.* 2016;64(12):2263-73.
25. Verkhratsky A, Matteoli M, Parpura V, Mothet JP, and Zorec R. Astrocytes as secretory cells of the central nervous system: idiosyncrasies of vesicular secretion. *EMBO J.* 2016;35(3):239-57.
26. Yin P, Knolhoff AM, Rosenberg HJ, Millet LJ, Gillette MU, and Sweedler JV. Peptidomic analyses of mouse astrocytic cell lines and rat primary cultured astrocytes. *J Proteome Res.* 2012;11(8):3965-73.
27. Tokay T, Hachem R, Masmoudi-Kouki O, Gandolfo P, Desrues L, Leprince J, Castel H, Diallo M, Amri M, Vaudry H, et al. Beta-amyloid peptide stimulates endozepine release in cultured rat astrocytes through activation of N-formyl peptide receptors. *Glia.* 2008;56(13):1380-9.
28. Loomis WF, Behrens MM, Williams ME, and Anjard C. Pregnenolone sulfate and cortisol induce secretion of acyl-CoA-binding protein and its conversion into endozepines from astrocytes. *The Journal of biological chemistry.* 2010;285(28):21359-65.
29. Guidotti A, Forchetti CM, Corda MG, Konkel D, Bennett CD, and Costa E. Isolation, characterization, and purification to homogeneity of an endogenous polypeptide with agonistic action on benzodiazepine receptors. *Proceedings of the National Academy of Sciences of the United States of America.* 1983;80(11):3531-5.
30. Farzampour Z, Reimer RJ, and Huguenard J. Endozepines. *Adv Pharmacol.* 2015;72:147-64.
31. Budry L, Bouyakdan K, Tobin S, Rodaros D, Marcher AB, Mandrup S, Fulton S, and Alquier T. DBI/ACBP loss-of-function does not affect anxiety-like behaviour but reduces anxiolytic responses to diazepam in mice. *Behav Brain Res.* 2016;313:201-7.
32. Bouyakdan K, Taib B, Budry L, Zhao S, Rodaros D, Neess D, Mandrup S, Faergeman NJ, and Alquier T. A novel role for central ACBP/DBI as a regulator of long-chain fatty acid metabolism in astrocytes. *Journal of neurochemistry.* 2015;133(2):253-65.
33. Lanfray D, Arthaud S, Ouellet J, Compere V, Do Rego JL, Leprince J, Lefranc B, Castel H, Bouchard C, Monge-Roffarello B, et al. Gliotransmission and brain glucose sensing: critical role of endozepines. *Diabetes.* 2013;62(3):801-10.
34. do Rego JC, Orta MH, Leprince J, Tonon MC, Vaudry H, and Costentin J. Pharmacological characterization of the receptor mediating the anorexigenic action of the octadecaneuropeptide: evidence for an endozepinergic tone regulating food intake. *Neuropsychopharmacology : official publication of the American College of Neuropsychopharmacology.* 2007;32(7):1641-8.
35. Wang Y, Hsuchou H, He Y, Kastin AJ, and Pan W. Role of Astrocytes in Leptin Signaling. *Journal of molecular neuroscience : MN.* 2015;56(4):829-39.
36. Heinrich G, Meece K, Wardlaw SL, and Accili D. Preserved energy balance in mice lacking FoxO1 in neurons of Nkx2.1 lineage reveals functional heterogeneity of FoxO1 signaling within the hypothalamus. *Diabetes.* 2014;63(5):1572-82.
37. Yee CL, Wang Y, Anderson S, Ekker M, and Rubenstein JL. Arcuate nucleus expression of NKX2.1 and DLX and lineages expressing these transcription factors in neuropeptide Y(+), proopiomelanocortin(+), and tyrosine hydroxylase(+) neurons in neonatal and adult mice. *J Comp Neurol.* 2009;517(1):37-50.
38. Fisette A, Tobin S, Decarie-Spain L, Bouyakdan K, Peyot ML, Madiraju SRM, Prentki M, Fulton S, and Alquier T. alpha/beta-Hydrolase Domain 6 in the Ventromedial Hypothalamus Controls Energy Metabolism Flexibility. *Cell Rep.* 2016;17(5):1217-26.
39. Alfonso J, Le Magueresse C, Zuccotti A, Khodosevich K, and Monyer H. Diazepam binding inhibitor promotes progenitor proliferation in the postnatal SVZ by reducing GABA signaling. *Cell stem cell.* 2012;10(1):76-87.
40. Benani A, Hryhorczuk C, Gouaze A, Fioramonti X, Brenachot X, Guissard C, Krezymon A, Duparc

T, Colom A, Nedelec E, et al. Food intake adaptation to dietary fat involves PSA-dependent rewiring of the arcuate melanocortin system in mice. *J Neurosci.* 2012;32(35):11970-9.
41. Vong L, Ye C, Yang Z, Choi B, Chua S, Jr., and Lowell BB. Leptin action on GABAergic neurons prevents obesity and reduces inhibitory tone to POMC neurons. *Neuron.* 2011;71(1):142-54.
42. Fioramonti X, Lorsignol A, Taupignon A, and Penicaud L. A new ATP-sensitive K+ channel-independent mechanism is involved in glucose-excited neurons of mouse arcuate nucleus. *Diabetes.* 2004;53(11):2767-75.
43. Gandolfo P, Patte C, Leprince J, Thoumas JL, Vaudry H, and Tonon MC. The stimulatory effect of the octadecaneuropeptide (ODN) on cytosolic Ca2+ in rat astrocytes is not mediated through classical benzodiazepine receptors. *European journal of pharmacology.* 1997;322(2-3):275-81.
44. Leprince J, Oulyadi H, Vaudry D, Masmoudi O, Gandolfo P, Patte C, Costentin J, Fauchere JL, Davoust D, Vaudry H, et al. Synthesis, conformational analysis and biological activity of cyclic analogs of the octadecaneuropeptide ODN. Design of a potent endozepine antagonist. *European journal of biochemistry / FEBS.* 2001;268(23):6045-57.
45. Chretien C, Fenech C, Lienard F, Grall S, Chevalier C, Chaudy S, Brenachot X, Berges R, Louche K, Stark R, et al. Transient Receptor Potential Canonical 3 (TRPC3) Channels Are Required for Hypothalamic Glucose Detection and Energy Homeostasis. *Diabetes.* 2017;66(2):314-24.
46. Adamsky A, Kol A, Kreisel T, Doron A, Ozeri-Engelhard N, Melcer T, Refaeli R, Horn H, Regev L, Groysman M, et al. Astrocytic Activation Generates De Novo Neuronal Potentiation and Memory Enhancement. *Cell.* 2018;174(1):59-71 e14.
47. Cai W, Xue C, Sakaguchi M, Konishi M, Shirazian A, Ferris HA, Li ME, Yu R, Kleinridders A, Pothos EN, et al. Insulin regulates astrocyte gliotransmission and modulates behavior. *The Journal of clinical investigation.* 2018;128(7):2914-26.
48. Alho H, Costa E, Ferrero P, Fujimoto M, Cosenza-Murphy D, and Guidotti A. Diazepam-binding inhibitor: a neuropeptide located in selected neuronal populations of rat brain. *Science.* 1985;229(4709):179-82.
49. Prevot V, Dehouck B, Sharif A, Ciofi P, Giacobini P, and Clasadonte J. The versatile tanycyte: a hypothalamic integrator of reproduction and energy metabolism. *Endocr Rev.* 2018;39(3):333-68.
50. Freire-Regatillo A, Argente-Arizon P, Argente J, Garcia-Segura LM, and Chowen JA. Non-Neuronal Cells in the Hypothalamic Adaptation to Metabolic Signals. *Frontiers in endocrinology.* 2017;8:51.
51. Siiskonen H, Oikari S, Korhonen VP, Pitkanen A, Voikar V, Kettunen M, Hakumaki J, Wahlfors T, Pussinen R, Penttonen M, et al. Diazepam binding inhibitor overexpression in mice causes hydrocephalus, decreases plasticity in excitatory synapses and impairs hippocampus-dependent learning. *Mol Cell Neurosci.* 2007;34(2):199-208.
52. Dumitru I, Neitz A, Alfonso J, and Monyer H. Diazepam Binding Inhibitor Promotes Stem Cell Expansion Controlling Environment-Dependent Neurogenesis. *Neuron.* 2017;94(1):125-37 e5.
53. Gerstner JR, Bremer QZ, Vander Heyden WM, Lavaute TM, Yin JC, and Landry CF. Brain fatty acid binding protein (Fabp7) is diurnally regulated in astrocytes and hippocampal granule cell precursors in adult rodent brain. *PLoS One.* 2008;3(2):e1631.
54. Yasumoto Y, Miyazaki H, Ogata M, Kagawa Y, Yamamoto Y, Islam A, Yamada T, Katagiri H, and Owada Y. Glial Fatty Acid-Binding Protein 7 (FABP7) Regulates Neuronal Leptin Sensitivity in the Hypothalamic Arcuate Nucleus. *Mol Neurobiol.* 2018;55(12):9016-28.
55. Guillebaud F, Girardet C, Abysique A, Gaige S, Barbouche R, Verneuil J, Jean A, Leprince J, Tonon MC, Dallaporta M, et al. Glial Endozepines Inhibit Feeding-Related Autonomic Functions by Acting at the Brainstem Level. *Front Neurosci.* 2017;11:308.
56. Ujjainwala AL, Courtney CD, Rhoads SG, Rhodes JS, and Christian CA. Genetic loss of diazepam binding inhibitor in mice impairs social interest. *Genes Brain Behav.* 2018;17(5):e12442.
57. Ujjainwala AL, Courtney CD, Wojnowski NM, Rhodes JS, and Christian CA. Differential impacts on multiple forms of spatial and contextual memory in diazepam binding inhibitor knockout mice. [published online ahead of print January 25, 2019]. *J Neurosci Res.* doi: 10.1002/jnr.24393.
58. Lanfray D, Caron A, Roy MC, Laplante M, Morin F, Leprince J, Tonon MC, and Richard D. Involvement of the Acyl-CoA binding domain containing 7 in the control of food intake and energy expenditure in mice. *Elife.* 2016;5:e11742.
59. Neess D, Bek S, Bloksgaard M, Marcher AB, Faergeman NJ, and Mandrup S. Delayed hepatic adaptation to weaning in ACBP-/- mice is caused by disruption of the epidermal barrier. *Cell Rep.* 2013;5(5):1403-12.

Figure 1

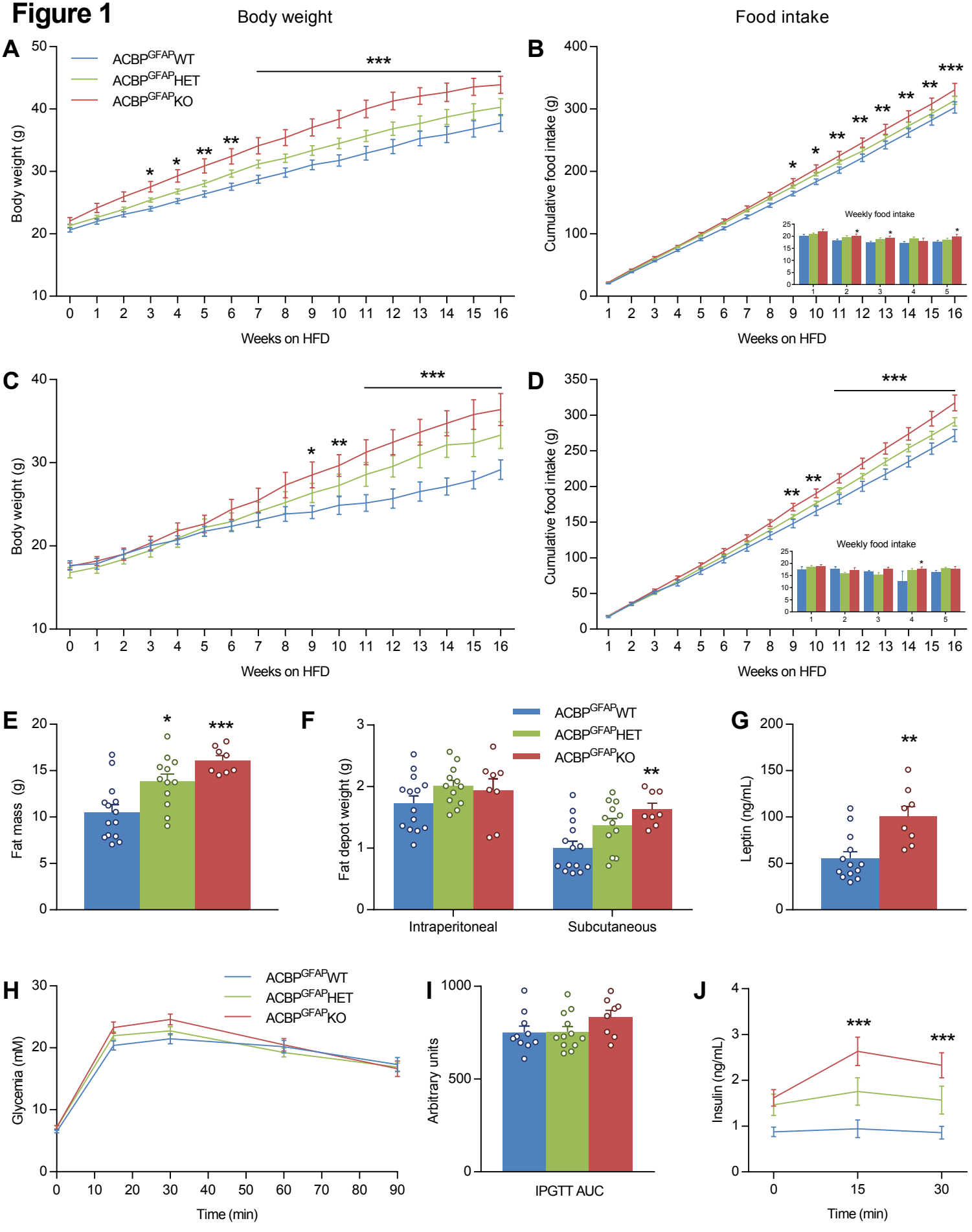
Body weight
Food intake
A
B
C
D
E
F
G
H
I
J
ACBP^GFAP WT
ACBP^GFAP HET
ACBP^GFAP KO
Body weight (g)
Weeks on HFD
Cumulative food intake (g)
Weekly food intake
Fat mass (g)
Fat depot weight (g)
Intraperitoneal
Subcutaneous
Leptin (ng/mL)
Glycemia (mM)
Time (min)
Arbitrary units
IPGTT AUC
Insulin (ng/mL)

Figure 1: Pan-brain astroglial ACBP deficiency promotes diet-induced obesity. Body weight and cumulative food intake of male **A-B** and female **C-D** ACBP^{GFAP} WT, HET and KO mice fed with a HFD during 16 weeks. Insets in **B** and **D** represent average weekly food intake. **E-** Fat mass, **F-** fat depot weights and **G-** fasting plasma leptin levels. **H-** Intra-peritoneal glucose tolerance test (1.5 g/kg), and **I-** area under the curve. **J-** Plasma insulin levels during the IPGTT. * $p<0.05$, ** $p<0.01$, *** $p<0.001$ compared to control littermates, Two-way ANOVA with Bonferroni post hoc test (**A-D** and **J**). * $p<0.05$, ** $p<0.01$, *** $p<0.001$ compared to controls, One-way ANOVA with Bonferroni post hoc test (**E** and **F**). ** $p<0.01$ compared to controls Student's *t*-test (**G)**. N=8-15 for male mice (**A, B, E-J**) and 6-7 for female mice (**C, D**).

Figure 2

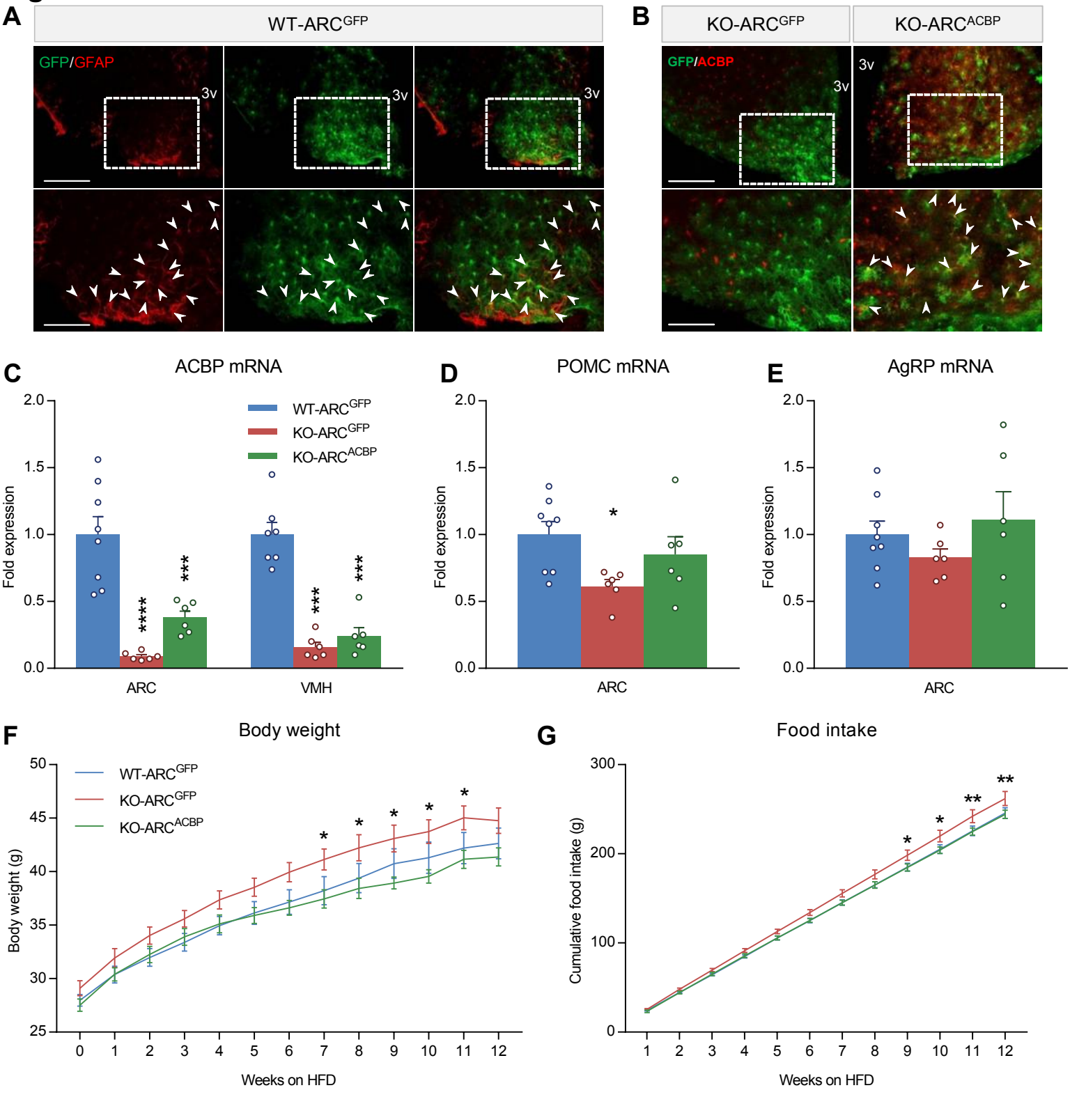
A
WT-ARC^GFP
GFP/GFAP
3v
B
KO-ARC^GFP
KO-ARC^ACBP
GFP/ACBP
C
ACBP mRNA
WT-ARC^GFP
KO-ARC^GFP
KO-ARC^ACBP
Fold expression
ARC
VMH
D
POMC mRNA
E
AgRP mRNA
F
Body weight
Body weight (g)
Weeks on HFD
G
Food intake
Cumulative food intake (g)

Figure 2: Genetic rescue of ACBP in GFAP-astrocytes of the ARC prevents DIO. A- Immunostaining of GFAP (red) and GFP (green) in GFAP-Cre mice injected with AAV expressing GFP under the control of the GFAP promoter in the ARC and **B-** ACBP (red) and GFP (green) in $ACBP^{GFAP}$ KO mice injected with GFP (left panel, KO-ARC^{GFP}) or ACBP (right panel, KO-ARC^{ACBP}) -expressing AAV in the ARC. White arrowheads indicates cells co-expressing GFAP and GFP (Panel **A**) and cells co-expressing ACBP and GFP (Panel **B**). Scale bar represents 100 µm in the top panels and 50 µm in zoomed panels (bottom). Representative images from 3 different mice. **C-** *acbp* expression measured by qPCR in ARC and VMH microdissections, **D-** *pomc* and **E-** *agrp* mRNA levels in ARC microdissections. * $p<0.05$, *** $p<0.001$, **** $p<0.0001$ compared to WT-ARC^{GFP}, One-way ANOVA with Bonferroni post hoc test, N=6-9. **F-** Body weight and **G-** cumulative food intake in animals fed with a HFD during 12 weeks. * $p<0.05$, ** $p<0.01$ KO-ARC^{ACBP} compared to KO-ARC^{GFP}, Two-way ANOVA with Bonferroni post hoc test, N=6-9.

Figure 3

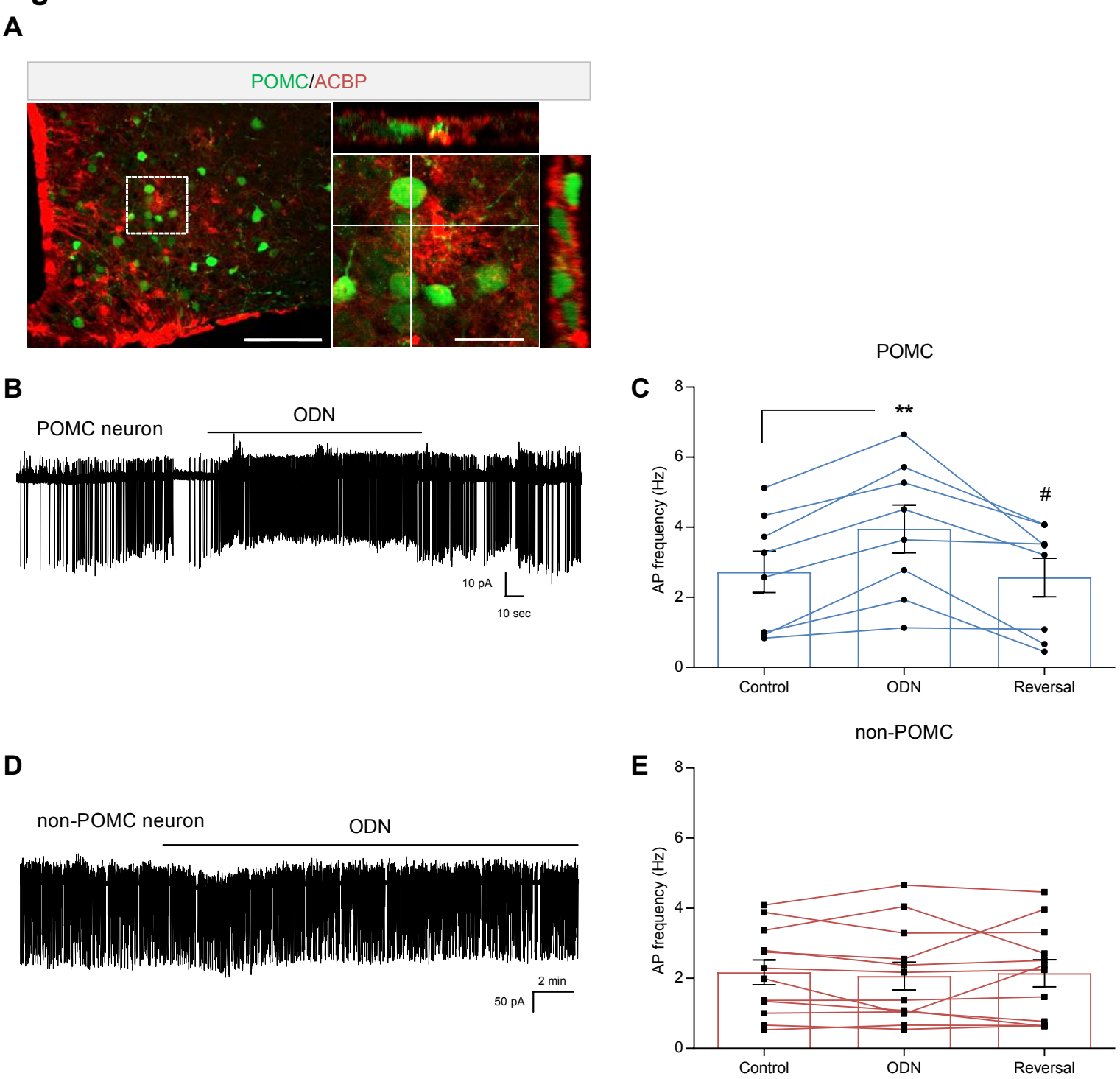
A
POMC/ACBP
B
POMC neuron
ODN
10 pA
10 sec
C
POMC
AP frequency (Hz)
**
#
Control
ODN
Reversal
D
non-POMC neuron
ODN
2 min
50 pA
E
non-POMC
AP frequency (Hz)
Control
ODN
Reversal

Figure 3: ODN selectively activates POMC neurons in the ARC. A- Immunostaining of ACBP-astrocytes (red) in close proximity to ARC POMC-eGFP neurons (green). Inset is represented with orthogonal projections. Scale bar represents 100 µm in the left panel and 25 µm in the inset. Representative images from 3 different mice. Representative trace and quantification of AP frequency in ARC POMC (**B**, **C**; N=8 neurons from 7 mice) or non-POMC (**D**, **E**; N=12 neurons from 7 mice) neurons in presence or absence of 1 nM ODN. ** $p<0.001$ compared to control and # $p<0.05$ compared to ODN, One-way ANOVA with repeated measures with Bonferroni post-hoc test.

Figure 4

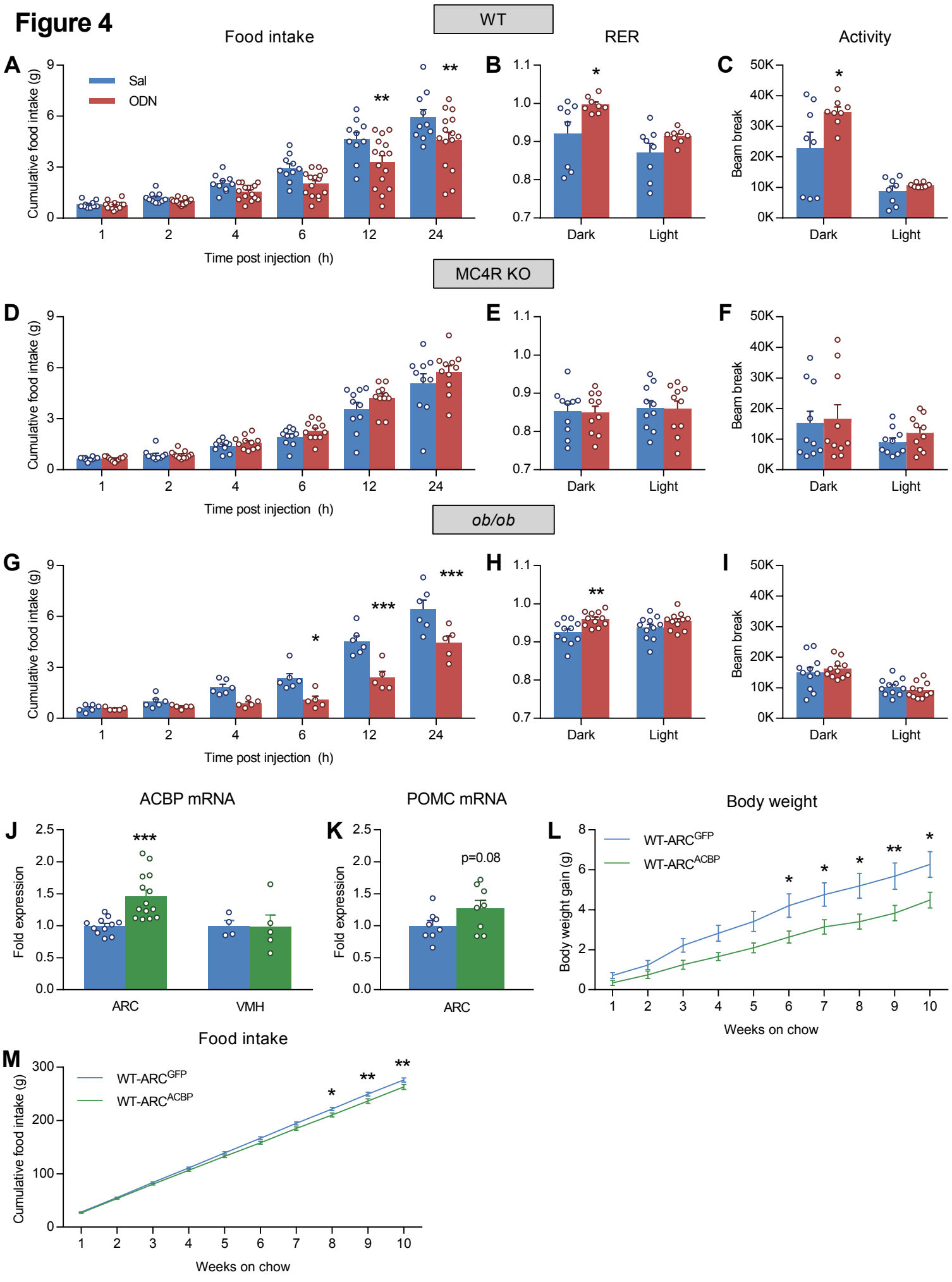
WT
Food intake
RER
Activity
A
B
C
Cumulative food intake (g)
Sal
ODN
Time post injection (h)
Beam break
Dark
Light
MC4R KO
D
E
F
ob/ob
G
H
I
ACBP mRNA
POMC mRNA
Body weight
J
K
L
Fold expression
ARC
VMH
p=0.08
WT-ARC^GFP
WT-ARC^ACBP
Body weight gain (g)
Weeks on chow
Food intake
M

Figure 4: Central effects of ODN on energy homeostasis rely on the melanocortin system. Cumulative food intake of **A-** C57BL/6J WT (N=10-15), **D-** MC4R KO (N=10-11) and **G-** *ob/ob* (N=5-6) overnight fasted (16 h) male mice following ICV administration of 100 ng of ODN or saline control. RER and locomotor activity in C57BL/6J WT **(B, C)**, MC4R KO **(E, F)** and *ob/ob* **(H, I)** mice measured in CLAMS metabolic cages during 24 h following ICV ODN or saline after 24 h acclimation. * $p<0.05$, ** $p<0.01$, *** $p<0.001$ compared to saline controls, Two-way ANOVA with Bonferroni post hoc test. **J-** *Acbp* expression measured by qPCR in ARC (N=11-14) and VMH (N=4-5) microdissections and **K-** *pomc* in ARC microdissections (N=8) from C57BL/6J WT male mice injected bilaterally in the ARC with AAV expressing GFP (WT-ARC^{GFP}) or ACBP (WT-ARC^{ACBP}) under the control of the GFAP promoter. *** $p<0.001$, Student's *t*-test compared to WT-ARC^{GFP}. **L-** Body weight gain and **M-** cumulative food intake in WT-ARC^{GFP} and WT-ARC^{ACBP} mice (N=12-15). * $p<0.05$, ** $p<0.01$, *** $p<0.001$ compared to WT-ARC^{GFP}, Two-way ANOVA with Bonferroni post hoc test.

Figure 5

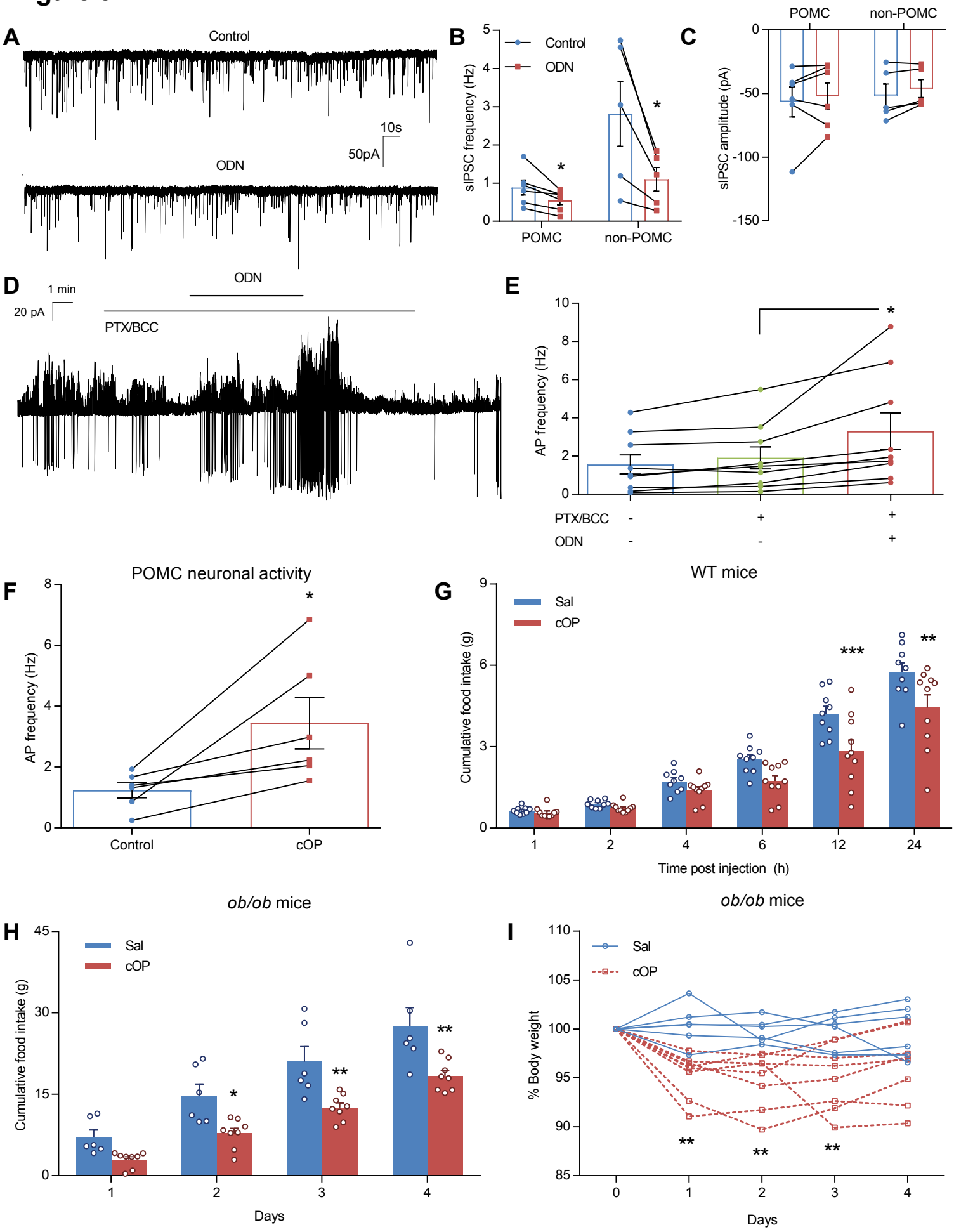
A
Control
10s
50pA
ODN
B
Control
ODN
sIPSC frequency (Hz)
POMC
non-POMC
C
POMC
non-POMC
sIPSC amplitude (pA)
D
1 min
20 pA
ODN
PTX/BCC
E
AP frequency (Hz)
PTX/BCC
ODN
F
POMC neuronal activity
AP frequency (Hz)
Control
cOP
G
WT mice
Sal
cOP
Cumulative food intake (g)
Time post injection (h)
ob/ob mice
H
Sal
cOP
Cumulative food intake (g)
Days
ob/ob mice
I
Sal
cOP
% Body weight
Days

Figure 5: ODN activates POMC neurons through a $GABA_A$ independent but ODN GPCR dependent mechanism. A- Representative voltage-clamp whole-cell recording of a POMC neuron with or without 1 nM ODN. **B-** Quantification of sIPSC frequency and **C-** amplitude of POMC and non-POMC neurons before and during ODN application. * $p<0.05$ compared to control, paired Student's *t*-test, N=5-6 neurons from 5-6 mice. **D-** Representative cell-attached recording of a POMC neuron in the presence of bicuculline, picrotoxin, Cnqx and APV before and during ODN application (1 nM). **E-** Quantification of AP frequency in POMC neurons with or without the inhibitors and ODN (1nM). * $p<0.05$ compared to inhibitors (ptx/bcc), One-way ANOVA repeated measures with Bonferroni post hoc test, N=10 neurons from 10 mice. **F-** Quantification of AP frequency of POMC neurons before and during $_C$OP (2 nM) application. * $p<0.05$, compared to control, paired Student's *t*-test, N=6 neurons from 4 mice. **G-** Cumulative food intake in overnight fasted (16 h) C57BL/6 WT male mice following ICV administration of 50 ng of $_C$OP or saline (N=9-10). **H-** Cumulative food intake and **I-** percent body weight change following daily ICV administration of 50 ng of $_C$OP or saline in *ad libitum* fed *ob/ob* mice (N=6-8). * $p<0.05$, ** $p<0.01$, *** $p<0.001$ compared to saline, Two-way ANOVA with Bonferroni post hoc test.